

Low-Pass Filter with Hybrid Integrator-Gain Switching for Increased Bandwidth

Marcel Heertjes^{*,**} and Yannick Knops^{**}

^{*} ASML, Mechatronic Systems Development, Veldhoven, The Netherlands

^{**} Eindhoven University of Technology, Department of Mechanical Engineering, Eindhoven, The Netherlands

Summary. In an attempt to surpass Bode's magnitude-phase relationship, the possibilities of a hybrid integrator-gain switching (HIGS) element are studied. The HIGS element has a describing function that combines a magnitude slope of minus 20 dB per decade with a phase lag of only 38.1 degrees, which is similar to the well-known Clegg integrator. Being integrated in second-order filters like low-pass or notch, the loopshaping design may significantly benefit from the phase advantage induced by the HIGS element. This will give rise to increased bandwidths, hence increased low-frequency disturbance rejection properties. To provide an objective comparison, the HIGS-based controller will be tuned by an autotuner. For given sensitivity bounds that meet robust stability requirements, a 20% increase of bandwidth is demonstrated when compared to its linear (and optimized) counterpart.

Introduction

Over the years control engineers and researchers alike have been intrigued by the idea of surpassing Bode's magnitude-phase relationship such as hinted at by the Clegg integrator [4]. That is, magnitude characteristics that show minus 20 dB per decade combined with a phase lag of only 38.1 degrees. Such properties should significantly aid the loopshaping design, especially since delay, which induces phase lag, is considered among the key limiters of said design. Reset control designs using Clegg integrators, however, suffer from two main deficiencies. First, the resets induce higher-order harmonics that often lead to high-frequency distortion in the presence of plant flexibilities [3]. Second, the closed-loop stability problem, which is generally posed in terms of linear matrix inequalities [5], is not particularly suited for small gain type of arguments. That is, the sector bounds of a reset element may require gains that become infinitely large [3]. As a result, graphical (frequency response based) stability tests like the circle criterion often become infeasible. To avoid these shortcomings, recently a hybrid integrator-gain switching element (further referred to as HIGS) has been proposed. In this paper, the HIGS element will be incorporated into a second-order low-pass filter and compared with a linear control design using an autotuner. The autotuner aims at maximum bandwidths while satisfying robust stability constraints on the magnitude of the closed-loop sensitivity functions.

Hybrid Integrator-Gain Switching (HIGS) Element

The HIGS element is a nonlinear controller element that switches between so-called gain mode ($k_h \geq 0$) and integrator mode ($\omega_h \geq 0$) depending on the system's state variables e , \dot{e} , and input u , or

$$\mathcal{H}(t, e) := \begin{cases} \dot{x}_h = \omega_h e, & \text{when } (e, u, \dot{e}) \in \mathcal{F}_1 \\ x_h = k_h e, & \text{when } (e, u, \dot{e}) \in \mathcal{F}_2 \\ u = x_h, & \end{cases} \quad \text{with} \quad \begin{cases} \mathcal{F}_1 := \left\{ (e, u, \dot{e}) \in \mathbb{R}^3 \mid eu \geq \frac{1}{k_h} u^2 \wedge (e, u, \dot{e}) \notin \mathcal{F}_2 \right\} \\ \mathcal{F}_2 := \left\{ (e, u, \dot{e}) \in \mathbb{R}^3 \mid u = k_h e \wedge \omega_h e^2 > k_h \dot{e} e \right\} \end{cases}. \quad (1)$$

In flow set \mathcal{F}_1 , the system is said to be in integrator mode. In flow set \mathcal{F}_2 , the system is said to be in gain mode. Note that the output $u(t)$, $t \in \mathbb{R}_{\geq 0}$ of the HIGS element $\mathcal{H}(t, e)$ evolves continuously but non-smooth from one flow set to the other. That is, in (1), we no longer make use of a jump set, *i.e.*, a jump of the output from one value to another as in [5]. In frequency domain, the HIGS element $\mathcal{H}(t, e)$ is given by its describing function:

$$\mathcal{D}(j\omega) = \frac{\omega_h}{j\omega} \left(\frac{\gamma}{\pi} + j \frac{e^{-2j\gamma} - 1}{2\pi} - 4j \frac{e^{-j\gamma} - 1}{2\pi} \right) + k_h \left(\frac{\pi - \gamma}{\pi} + j \frac{e^{-2j\gamma} - 1}{2\pi} \right) \quad \text{with } \gamma = 2\arctan\left(\frac{k_h \omega}{\omega_h}\right), \quad (2)$$

i.e., the harmonic contribution of the nonlinear element $\mathcal{H}(t, e)$ in (1) subject to an harmonic input $e(t) = \sin(\omega t)$. Apart from the gain k_h , (2) clearly shows low-pass characteristics. Namely, for $\omega \rightarrow 0$, *i.e.*, $\gamma \rightarrow 0$, $\mathcal{D}(j\omega) \rightarrow k_h$, whereas for $\omega \rightarrow \infty$, *i.e.*, $\gamma \rightarrow \pi$, $\mathcal{D}(j\omega) \rightarrow (\omega_h/j\omega)(1 - 4j/\pi)$, which equals the Clegg integrator [4]. To assess the phase advantage of the HIGS element $\mathcal{H}(t, e)$ in (1), such as implied by the describing function in (2), $\mathcal{H}(t, e)$ is put in front of a linear first-order low pass filter [2]. The result will be a second-order low-pass filter whose describing function (along with the linear low-pass filter $\mathcal{C}_{lp}(j\omega)$ with cut-off frequency $\omega_{lp} \geq 0$) is given by

$$\mathcal{D}_{lp}(j\omega) = \mathcal{D}(j\omega) \mathcal{C}_{lp}(j\omega) \quad \text{with} \quad \mathcal{C}_{lp}(j\omega) = \frac{\omega_{lp}}{j\omega + \omega_{lp}}. \quad (3)$$

Loopshaping Control Design

In a loopshaping control context, the HIGS-based low-pass filter, whose describing function is given by (3), will be used as a substitute for a linear second-order low-pass filter; the latter will be denoted by $\mathcal{C}_{lp}^*(j\omega)$. Note that $\mathcal{C}_{lp}^*(j\omega) \neq \mathcal{C}_{lp}(j\omega) \mathcal{C}_{lp}(j\omega)$ and thus has the possibility of having complex poles, which is not the case for the currently chosen HIGS-based low-pass filter, see also [2]. The second-order low-pass filters, either HIGS-based or simply linear, will

be used in series connection with a PID controller \mathcal{C}_{pid} to control an industrial wafer stage plant \mathcal{P} . Plant \mathcal{P} has the properties of a floating mass system, *i.e.*, 40 dB per decade magnitude decay and a phase lag of 180 degrees. It also contains high-frequency resonances that potentially compromise robust stability of the control design and (as such) can lead to bandwidth limitations. The frequency response functions of both plant $\mathcal{P}(j\omega)$ and controllers $\mathcal{C}_1(j\omega) = \mathcal{C}_{pid}(j\omega)\mathcal{C}_{lp}^*(j\omega)$ and $\mathcal{C}_2(j\omega) = \mathcal{C}_{pid}(j\omega)\mathcal{D}_{lp}(j\omega)$ are input to an autotuner that has the possibility of tuning all of the linear controller parameters with the aim to maximize bandwidth under robust stability constraints. The tuning of the HIGS parameters k_h and ω_h is part of an iterative (and manual) tuning process. The result of autotuner regarding the linear control design can therefore be considered optimal, but the result of the HIGS-based control design cannot and may be subject to further improvement. Robust stability requirements are mainly imposed on the closed-loop sensitivity function, which until 1kHz is not allowed to peak beyond 10 dB, *i.e.*, the so-called S-circle. Beyond 1 kHz, peaking is constrained at 3 dB, *i.e.*, the so-called SH-circle. Closed-loop stability of the (optimized) loop transfer with autotuner will be iteratively checked using Nyquist's criterion. For the HIGS-based control design, the loop transfer will be based on the describing function $\mathcal{D}_{lp}(j\omega)$ in (3). As such, no conclusive statements can be made regarding stability of the closed-loop system when using the HIGS element $\mathcal{H}(t, e)$ as defined in (1). The results of autotuner are shown in the left part of Figure 1. For the linear control design a maximum bandwidth is obtained of 316 Hz. Using the HIGS-based

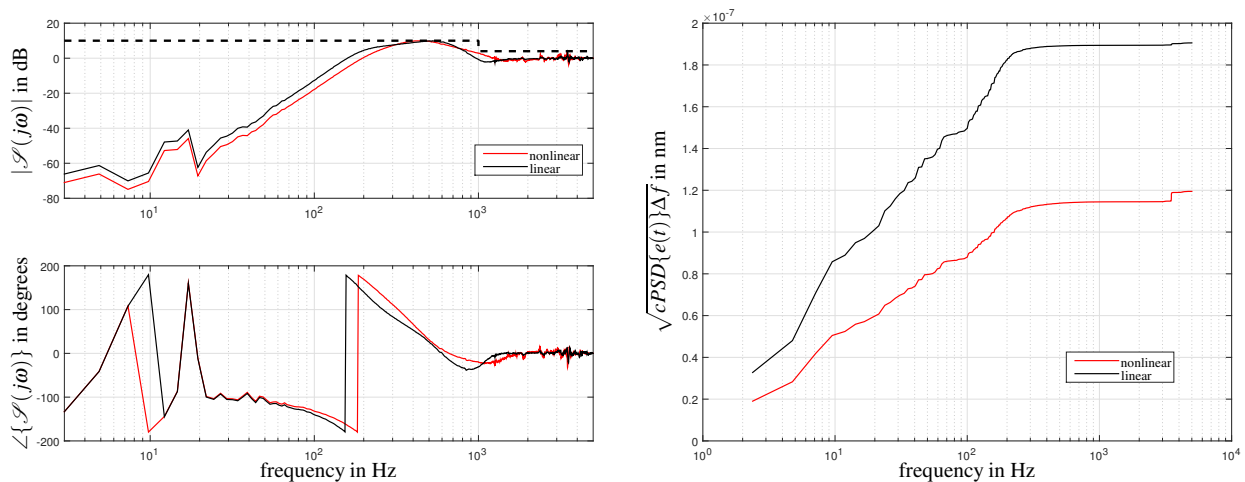


Figure 1: (left) Bode diagrams with sensitivity bounds, and (right) cumulative power spectral densities (PSDs).

low-pass filter, the bandwidth could be increased up to 376 Hz, hence almost 20% improvement. The higher bandwidth gives rise to improved low-frequency disturbance suppression. This is shown in the right part of Figure 1. For either the closed-loop system based on the HIGS element $\mathcal{H}(t, e)$ in (1) or its linear counterpart, the figure shows the result of time-domain simulations, which are evaluated by cumulative power spectral densities (PSDs). Under realistic disturbances, the increased bandwidth induces an increase of low-frequency disturbance suppression. At the same time, the high-frequency noise distortion due to HIGS remains fairly limited.

Remark On Closed-Loop Stability

For a rigorous result on closed-loop stability, consider the loop transformed system $\tilde{\mathcal{H}}(t, e)$, which is similar to system $\mathcal{H}(t, e)$ in (1), but whose output $\tilde{u}(t)$ is given by $\tilde{u}(t) = u(t) - 0.5k_h e(t)$. It holds that $\|\tilde{\mathcal{H}}(t, e)\|_2 \leq \gamma_1 \|e(t)\|_2$ with $\gamma_1 = 0.5k_h$. For the linear time-invariant system interconnected with $\tilde{\mathcal{H}}(t, e)$, define $\gamma_2 = \sup_{\omega \in \mathbb{R}} \|\mathcal{O}_l(j\omega)/(1 + 0.5k_h \mathcal{O}_l(j\omega))\|_2$ with the loop transfer $\mathcal{O}_l(j\omega) := \mathcal{C}_{lp}(j\omega)\mathcal{C}_{pid}(j\omega)\mathcal{P}(j\omega)$. By applying the small-gain theorem [1], it follows that the HIGS-based closed-loop system is finite gain \mathcal{L} stable if $\gamma_1 \gamma_2 < 1$, which is satisfied for $\gamma_2 < 2/k_h$.

Conclusion

A nonlinear low-pass filter design is presented that offers the possibility of increased bandwidths unattainable to its linear counterpart. The findings could lead to a full nonlinear loopshaping design by replacing integrators with HIGS elements.

References

- [1] Desoer C.A., Vidyasagar M. (1975) Feedback systems: input-output properties. Academic Press, NY.
- [2] Hazeleger L., Heertjes, M.F., Nijmijer H. (2016) Second-order reset elements for stage control design. *American Control Conference*, Boston, MA:2643-2648.
- [3] Heertjes M.F., Gruntjens K.G.J., Van Loon S.J.L.M., Van de Wouw N., Heemels W.P.M.H. (2016) Experimental evaluation of reset control for improved stage performance. *IFAC-PapersOnLine* 49-13, 93-98.
- [4] Chait Y., Hollot C.V. (2002) On Horowitz's contributions to reset control. *International Journal of Robust and Nonlinear Control*, **12**:335-355.
- [5] Zaccarian L., Nešić D., Teel A.R. (2011) Analytical and numerical Lyapunov functions for SISO linear control systems with first-order reset elements. *International Journal of Robust and Nonlinear Control*, **21**:1134-1158.